Stamp Collapse in Soft Lithography

Yonggang Y. Huang,*,† Weixing Zhou,† K. J. Hsia,‡ Etienne Menard,§,∥ Jang-Ung Park,§ John A. Rogers,§ and Andrew G. Alleyne†

Department of Mechanical and Industrial Engineering, Department of Theoretical and Applied Mechanics, and Department of Materials Science and Engineering, University of Illinois at Urbana-Champaign, Urbana, Illinois 61801, and Laboratoire de Chimie Organique, UMR 7611, Université Pierre et Marie Curie, 4 place Jussieu, F-75252 Paris, France

Received January 25, 2005. In Final Form: May 5, 2005

We have studied the so-called roof collapse in soft lithography. Roof collapse is due to the adhesion between the PDMS stamp and substrate, and it may affect the quality of soft lithography. Our analysis accounts for the interactions of multiple punches and the effect of elastic mismatch between the PDMS stamp and substrate. A scaling law among the stamp modulus, punch height and spacing, and work of adhesion between the stamp and substrate is established. Such a scaling law leads to a simple criterion against the unwanted roof collapse. The present study agrees well with the experimental data.

1. Introduction

Soft lithography is an important method for micro- and nanofabrication and has many applications in plastic electronics and fiber optics.[1−6] Figure 1 shows a schematic diagram of an elastomeric stamp on a substrate in soft lithography. The stamp surface consists of flat punches whose width $2w$ is on the order of micrometers or larger. The punch height h ranges from micrometers to several hundred nanometers or even smaller, whereas punch spacing $2a$ also has a large variation. The ink is applied to the stamp with a pattern of surface relief shown in Figure 1, and ink is transferred to the substrate when the stamp is brought into contact with the substrate. The elastomeric stamp is usually made of poly(dimethylsiloxane) (PDMS), which is very compliant and has a low shear modulus μ of less than 1 MPa. This low stiffness makes PDMS easily deformable, which may affect the quality of soft lithography.

Hui et al.[7] studied various deformation mechanisms of the stamp, such as the punch buckling, lateral collapse, and roof collapse. Here roof collapse represents the collapse of the stamp toward the substrate as shown schematically in Figure 1. Hui et al.[7] obtained the critical external load $(\sigma_0)_{critical}$ for roof collapse in terms of the Young's modulus of the stamp and punch geometry (height, width, and spacing). Once the external load σ_0 reaches $(\sigma_0)_{critical}$, roof collapse occurs and yields unwanted contact between the sagged surfaces of the stamp and the substrate.

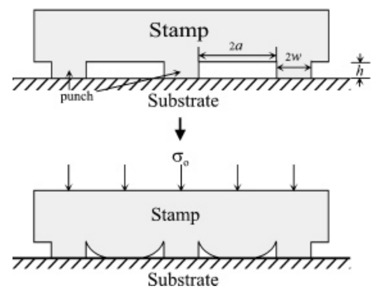

Figure 1. Schematic diagrams of the stamp on a substrate in soft lithography and roof collapse due to external load σ_0. The punches of the stamp have width $2w$, height h, and spacing $2a$.

Roof collapse has been observed in recent experiments of Sharp et al.[8] for small punch height h ($\ll$punch width $2w$ and spacing $2a$, Figure 1). Sharp et al.[8] attributed roof collapse to (1) the external load that placed the sagged surfaces of the stamp in contact with the substrate and (2) the adhesion between the stamp and substrate, which kept them in contact. Recent experiments[9] have shown that, for very small punch height, roof collapse may occur without any external load (i.e., $\sigma_0 = 0$). Furthermore, roof collapse is not due to the self-weight of the stamp because the roof of the stamp can collapse onto the substrate (in a similar way) even when the specimen is flipped (i.e., the stamp underneath the substrate). Roof collapse without the external load is due to the adhesion between the stamp and substrate.

The purposes of this paper are to analyze roof collapse without external load and to establish a criterion against the unwanted roof collapse in soft lithography. We develop a micromechanics model for roof collapse that leads to a scaling law among the stamp modulus, punch geometry (height h, width $2w$, spacing $2a$), and work of adhesion between the stamp and substrate. This scaling law gives a simple criterion for roof collapse, which states that roof collapse occurs once the punch height is below a critical

† Department of Mechanical and Industrial Engineering, University of Illinois at Urbana-Champaign.

‡ Department of Theoretical and Applied Mechanics, University of Illinois at Urbana-Champaign.

§ Department of Materials Science and Engineering, University of Illinois at Urbana-Champaign.

∥ Université Pierre et Marie Curie.

(1) Xia, Y.; Whitesides, G. *Angew. Chem., Int. Ed.* **1998**, *37*, 551−575.
(2) Xia, Y.; Rogers, J. A.; Paul, K. E.; Whitesides, G. M. *Chem. Rev.* **1999**, *99*, 1823−1848.
(3) Mirkin, C. A.; Rogers, J. A. *MRS Bull.* **2001**, *26*, 506.
(4) Loo, Y.-L.; Someya, T.; Baldwin, K. W.; Ho, P.; Bao, Z.; Dodabalapur, A.; Katz, H. E.; Rogers, J. A. *Proc. Natl. Acad. Sci. U.S.A.* **2002**, *99*, 10252−10256.
(5) Zaumseil, J.; Meitl, M. A.; Hsu, J. W. P.; Acharya, B.; Baldwin, K. W.; Loo, Y.-L.; Rogers, J. A. *Nano Lett.* **2003**, *3*, 1223−1227.
(6) Sundar, V. C.; Zaumseil, J.; Menard, E.; Podzorov, V.; Someya, T.; Gershenson, M.; Rogers, J. A. *Science* **2004**, *303*, 1644−1646.
(7) Hui, C. Y.; Jagota, A.; Lin, Y. Y.; Kramer, E. J. *Langmuir* **2002**, *18*, 1394−1407.
(8) Sharp, K. G.; Blackman, G. S.; Glassmaker, N. J.; Jagota, A.; Hui, C. Y. *Langmuir* **2004**, *20*, 6430−6438.
(9) Hsia, K. J.; Huang, Y.; Menard, E.; Park, J.-U.; Zhou, W.; Rogers, J. A.; Fulton, J. M. *Appl. Phys. Lett.* **2005**, *86*, 154106.

10.1021/la0502185 CCC: $30.25
Published on Web 06/29/2005

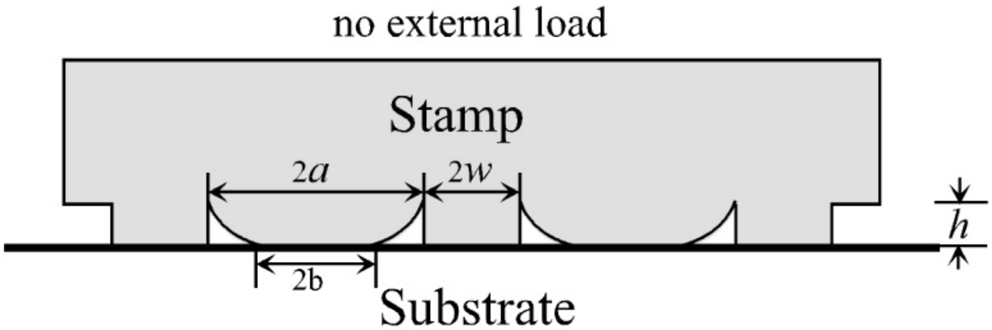

Figure 2. Schematic diagram of roof collapse (collapse of the stamp onto the substrate) due to the adhesion between the stamp and substrate without an external load (i.e., $\sigma_0 = 0$ in Figure 1). The width, height, and spacing of the punch are $2w$, h and $2a$, respectively. The collapse length is denoted by $2b$.

value, and this critical value is given analytically in terms of the stamp modulus, punch spacing and width, and work of adhesion between the stamp and substrate. This simple criterion is useful for soft lithography against the unwanted roof collapse.

This paper is structured as follows. We develop the method in section 2 to compute the total potential energy, which consists of the deformation energy and the adhesion energy due to roof collapse. Because the punch height h is much smaller than the punch spacing $2a$, the gaps between the stamp and substrate are modeled as microcracks. To illustrate this approach, we study the limit of small punch spacing in section 3 (i.e., punch width $2w \gg$ punch spacing $2a$ ($\gg$ punch height h)). A scaling law is established that involves the punch spacing $2a$ and height h, stamp modulus E, and work of adhesion γ between the stamp and substrate. The unsagged length of the stamp during roof collapse is obtained in section 3, and it will be used in section 6 to determine the work of adhesion from experiments. Section 4 gives an approximate analysis for multiple punches with width $2w$ and spacing $2a$. The effect of elastic mismatch between the stamp and substrate is accounted for in section 5, and a simple design criterion against unwanted roof collapse is also established. The unsagged length, accounting for effects of multiple punches and elastic mismatch between the PDMS stamp and substrate, is compared with the experimental data in section 6.

2. Model of Roof Collapse in Soft Lithography

The schematic diagram in Figure 2 shows roof collapse in soft lithography due to the adhesion between the stamp and substrate. Contrary to Figure 1, there is no external load such that roof collapse is completely due to the adhesion between the sagged part of the stamp and substrate. The work of adhesion γ is given by $\gamma = \gamma_{\mathrm{PDMS}} + \gamma_{\mathrm{substrate}} - \gamma_{\mathrm{int}}$, where γ_{PDMS} and $\gamma_{\mathrm{substrate}}$ are the surface energy of the PDMS stamp and substrate, respectively, and γ_{int} is the energy of the PDMS/substrate interfaces.

For a small punch height $h \ll$ punch width $2w$ and spacing $2a$, the roof will collapse onto the substrate if the collapsed state has a lower state of energy. We define the uncollapsed state as the ground state (of zero energy). The total potential energy associated with roof collapse is given by

$$U_{\mathrm{total}} = U_{\mathrm{deformation}} - 2b\gamma \tag{1}$$

where $U_{\mathrm{deformation}}$ is the deformation energy, γ is the work of adhesion between the stamp and substrate, and $2b$ is the collapse length (Figure 2) to be determined. Here U_{total} and $U_{\mathrm{deformation}}$ are the energy per punch for the periodic structure in Figure 2. The deformation energy $U_{\mathrm{deformation}}$ scales with h^2 for linear elastic deformation and becomes negligible for $h \to 0$ such that the total potential energy becomes negative and less than that (zero) for the uncollapsed state, which is the reason for roof collapse.

In the following, we first neglect the mismatch in the elastic moduli between the stamp and substrate and model them as a homogeneous material. The effect of elastic mismatch will be accounted for in section 5. Without losing generality, our analysis is two-dimensional (i.e., for a unit thickness in the out-of-plane direction). The PDMS is incompressible with the Poisson ratio $\nu = 0.5$. Let E denote the Young's modulus of PDMS, and its plane-strain modulus $E' = E/(1 - \nu^2) = 4/3E$.

Figure 3 shows our model to calculate the deformation energy $U_{\mathrm{deformation}}$ via the principle of linear superposition. The collapsed state with collapse length $2b$ can be considered to be the *difference* between

(i) the ground state without the collapse and

(ii) a constant *opening* displacement h over the length $2b$ around the center of each gap, as shown schematically in Figure 3. The difference between i and ii ensures the conditions of the collapsed state (i.e., the opening at the center portion (of length $2b$) is zero; the opening at the ends is h; and the unsagged portions remain traction-free). The ground state (i) has zero energy (and also zero stress and strain). Because the punch height is much smaller than punch spacing, $h \ll a$, we may approximate each gap as a crack, as shown by state iii in Figure 3. In other words, ii becomes a state of coplanar periodic cracks with crack length (= punch spacing) $2a$, crack spacing (= punch width) $2w$, and constant crack opening h over length $2b$ around the center of each crack. The deformation energy is then obtained from states i and iii as

$$U_{\mathrm{deformation}} = -\frac{1}{2}\int_{\mathrm{crack\ face}} \sigma_{yy} h \, \mathrm{d}x = \frac{E'h^2}{4} f\!\left(\frac{b}{a}, \frac{w}{a}\right) \tag{2}$$

where σ_{yy} is the normal stress on the crack face and f is a nondimensional function to be determined. The total potential energy in eq 1 becomes

$$U_{\mathrm{total}} = \frac{E'h^2}{4}\left[f\!\left(\frac{b}{a}, \frac{w}{a}\right) - \frac{8a\gamma}{E'h^2}\frac{b}{a}\right] \tag{3}$$

Collapse length $2b$ is determined by minimizing the above total potential energy

$$\frac{\partial U_{\mathrm{total}}}{\partial b} = 0 \tag{4}$$

which gives the normalized collapse length b/a in terms of the punch width/spacing ratio w/a and the normalized work of adhesion $8a\gamma/E'h^2$.

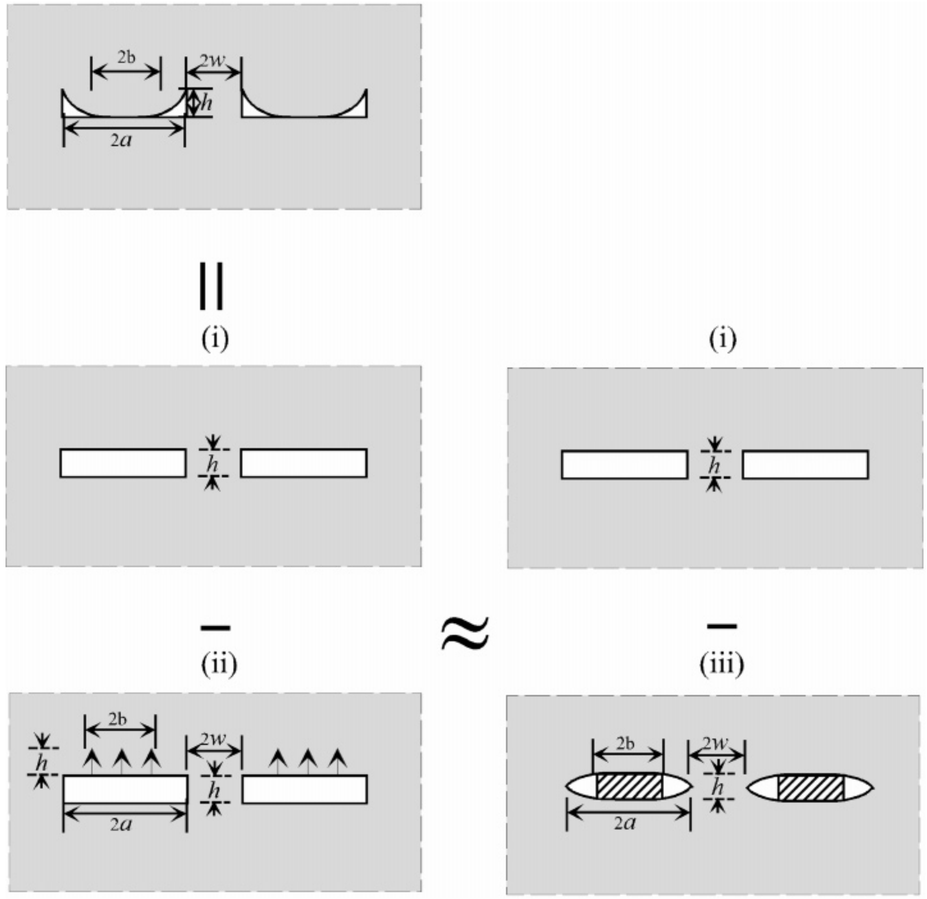

Figure 3. Schematic diagram to illustrate roof collapse as the difference between the ground state and the state of periodic gaps subject to a constant opening displacement h over the length $2b$ around the center of each gap. The latter can be approximated by coplanar, periodic cracks with crack length $2a$, crack spacing $2w$, and constant crack opening h over a length $2b$ on each crack.

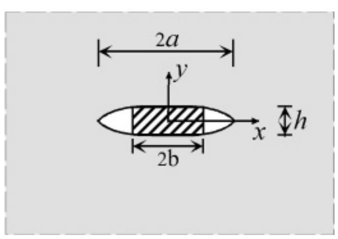

Figure 4. Schematic diagram for the limit of small punch spacing, which is modeled as a single crack with crack length $2a$ and constant crack opening h over a length $2b$. The origin of the Cartesian coordinate is at the center of the crack.

3. Limit of Small Punch Spacing: $2a \ll 2w$

We first consider the limit of small punch spacing $a \ll w$ (but $a \gg h$ still holds). This limit corresponds to closely packed punches. We do not account for the effect of elastic mismatch between the PDMS stamp and substrate in this section in order to obtain a simple analytical solution that leads to a scaling law. Such an effect will be considered in section 5. Therefore, the results in section 5 should be used to compare with the experiments because PDMS and the substrate have a large elastic mismatch.

Under this limit, $2w \gg 2a \gg h$, the last figure in Figure 3 becomes a single crack of length $2a$ with a constant opening h over the central portion of length $2b$ in an infinite body, as shown schematically in Figure 4. The Cartesian coordinates are set at the center of the crack.

The shear stress σ_{xy} vanishes on the entire crack plane because of symmetry. There are three different boundary conditions on the crack plane, namely,

(i) a symmetry condition outside the crack, $u_y = 0$ for $y = 0$, $|x| > a$,

(ii) a traction-free condition away from the center of the crack $\sigma_{yy} = 0$ for $y = 0$, $a > |x| > b$, and

(iii) a constant opening condition around the center of the crack, $\Delta u_y = h$ for $y = 0$, $b > |x|$,

where u_y is the displacement and $\Delta u_y = u_y^+ - u_y^-$ is the crack opening. The analytical solution for this problem can be found in Tada et al.[10] In particular, the normal stress σ_{yy} on the crack face is given by

$$\sigma_{yy}|_{y=0} = \begin{cases} \dfrac{-E'ha}{4K\left(\sqrt{1-\dfrac{b^2}{a^2}}\right)\sqrt{(a^2-x^2)(b^2-x^2)}}, & |x| < b \\ 0, & b < |x| < a \end{cases} \tag{5}$$

where $E' = 4/3E$, E is the Young's modulus of the stamp, and K is the complete elliptic integral of first kind given by

$$K(k) = \int_0^{\pi/2} \frac{\mathrm{d}\phi}{\sqrt{1-k^2\sin^2\phi}} \tag{6}$$

(10) Tada, H.; Paris, P. C.; Irwin, G. R. *The Stress Analysis of Cracks Handbook*, 3rd ed.; ASME Press: New York, 2000.

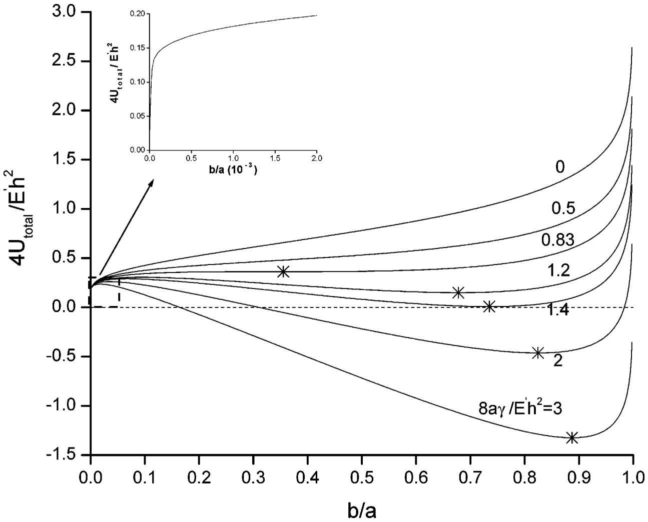

Figure 5. Normalized total potential energy $4U_{\text{total}}/E'h^2$ versus normalized collapse length b/a for the limit of small punch spacing, where $E' = {}^4/_3E$ is the plane-strain modulus of the PDMS stamp (E is Young's modulus), h and $2a$ are the punch height and spacing, respectively, and $2b$ is the collapse length. Several values of the normalized work of adhesion $8a\gamma/E'h^2$ are taken, where γ is the work of adhesion between the stamp and substrate. The inset shows $4U_{\text{total}}/E'h^2$ vs $8a\gamma/E'h^2$ for small b/a. The state of minimal total potential energy is marked by * on each curve (if applicable). The horizontal dashed line represents the uncollapsed state ($U_{\text{total}} = 0$).

with limits of $K(0) = \pi/2$ and $K(k \to 1) \approx -{}^1/_2\ln(1 - k^2)$. The substitution of eq 5 into eq 2 gives the deformation energy as

$$U_{\text{deformation}} = \frac{E'h^2}{4}\frac{K\left(\frac{b}{a}\right)}{K\left(\sqrt{1-\frac{b^2}{a^2}}\right)} \tag{7}$$

The total potential energy in eq 3 is then given by

$$U_{\text{total}} = \frac{E'h^2}{4}\left[\frac{K\left(\frac{b}{a}\right)}{K\left(\sqrt{1-\frac{b^2}{a^2}}\right)} - \frac{8a\gamma}{E'h^2}\frac{b}{a}\right] \tag{8}$$

The total potential energy, after being normalized by $E'h^2/4$, depends on the normalized collapse length b/a and normalized work of adhesion $8a\gamma/E'h^2$. This nondimensional parameter $8a\gamma/E'h^2$, which has also been identified by Sharp et al.,[8] represents the ratio of the adhesion energy ($\sim 2a\gamma$) to the deformation energy ($\sim {}^1/_4E'h^2$). It suggests a scaling law among the work of adhesion, stamp modulus, and punch spacing and height. In other words, stamp collapse is controlled by this combination of material and geometry parameters, $8a\gamma/E'h^2$.

Figure 5 shows the normalized total potential energy $4U_{\text{total}}/E'h^2$ versus the normalized collapse length b/a for the normalized work of adhesion $8a\gamma/E'h^2 = 0$, 0.5, 0.83, 1.2, 1.4, 2, and 3, where $8a\gamma/E'h^2 = 0$ corresponds to the limit of no adhesion between the stamp and substrate and the corresponding curve increases monotonically with b/a. The inset in Figure 5 shows that the total potential energy U_{total} is indeed zero for $b/a = 0$ (i.e., no collapse). For the other limit $b/a \to 1$ (i.e., complete collapse), U_{total} becomes unbounded.

There are several states of roof collapse that are controlled by $8a\gamma/E'h^2$. For $8a\gamma/E'h^2 < 0.83$ (weak adhesion), the curves increase monotonically with b/a such that U_{total} does not have a minimum. Therefore, roof collapse will not occur if the work of adhesion is low. In other words, if the roof is forced to collapse onto the substrate, then the roof will "spring back" as soon as the force is removed. For $8a\gamma/E'h^2 > 0.83$ (intermediate or strong adhesion), each curve in Figure 5 has a minimum (marked by * in Figure 5). Roof collapse may occur in order to reach this state of minimal total potential energy. In other words, if the roof is forced to collapse onto the substrate, then the roof may stay in the collapsed state after the force is removed. The corresponding collapse length at which U_{total} reaches the minimum is denoted by $2b_{\text{critical}}$. The minimal total potential energy $U_{\text{total}}^{\min}$ of the collapsed state is given by

$$U_{\text{total}}^{\min} = \frac{E'h^2}{4}\left[\frac{K\left(\frac{b_{\text{critical}}}{a}\right)}{K\left(\sqrt{1-\frac{b_{\text{critical}}^2}{a^2}}\right)} - \frac{8a\gamma}{E'h^2}\frac{b_{\text{critical}}}{a}\right] \tag{9}$$

For $0.83 < 8a\gamma/E'h^2 < 1.40$ (intermediate adhesion), $U_{\text{total}}^{\min}$ is positive, which gives the minimal total potential energy (marked by * in Figure 5) above the horizontal dashed line of $U_{\text{total}} = 0$ in Figure 5. The energy of the collapsed state for $0.83 < 8a\gamma/E'h^2 < 1.40$ is higher than that for the uncollapsed state $U_{\text{total}} = 0$ (ground state). Therefore, even though roof collapse may occur, it is unstable because some disturbances in the environment may reverse it back to the uncollapsed state. For $8a\gamma/E'h^2 > 1.40$ (strong adhesion), $U_{\text{total}}^{\min}$ is negative, and the minimal energy (marked by * in Figure 5) is lower than the horizontal dashed line for $U_{\text{total}} = 0$ in Figure 5 such that the collapsed state is stable.

These three states of no collapse, metastable collapse, and stable collapse are further explained in Figure 6, which shows the minimal total potential energy $4U_{\text{total}}^{\min}/E'h^2$ versus the normalized work of adhesion $8a\gamma/E'h^2$. These three states correspond to weak adhesion ($8a\gamma/E'h^2 < 0.83$), intermediate adhesion ($0.83 < 8a\gamma/E'h^2 < 1.40$), and strong adhesion ($8a\gamma/E'h^2 > 1.40$), respectively.

Figure 7 shows the normalized collapse length, b_{critical}/a, versus the normalized work of adhesion $8a\gamma/E'h^2$. For $8a\gamma/E'h^2 < 0.83$, collapse does not occur, and there is no solution for b_{critical}. For $0.83 < 8a\gamma/E'h^2 < 1.40$, there is a solution for b_{critical}, but roof collapse is unstable. The collapse length ranges from $b_{\text{critical}}/a = 0.35$ (for $8a\gamma/E'h^2 = 0.83$) to 0.74 (for $8a\gamma/E'h^2 = 1.40$). This suggests that once roof collapse occurs the collapse length is at least 35% of the punch spacing. In other words, for $8a\gamma/E'h^2$ across 0.83 (from $0.83 - \epsilon$ to $0.83 + \epsilon$, $\epsilon \to 0^+$), the collapse length jumps from zero (i.e., no collapse) to 35% of the punch spacing $2a$. For $8a\gamma/E'h^2 > 1.40$, roof collapse is stable, and the collapse length is at least 74% of punch spacing $2a$. For large $8a\gamma/E'h^2$, the collapse length approaches punch spacing $2a$ asymptotically.

As illustrated in Figure 3, the opening displacement after roof collapse is the difference between constant opening h over length $2a$ (of the punch spacing) and that associated with constant opening h over center portion

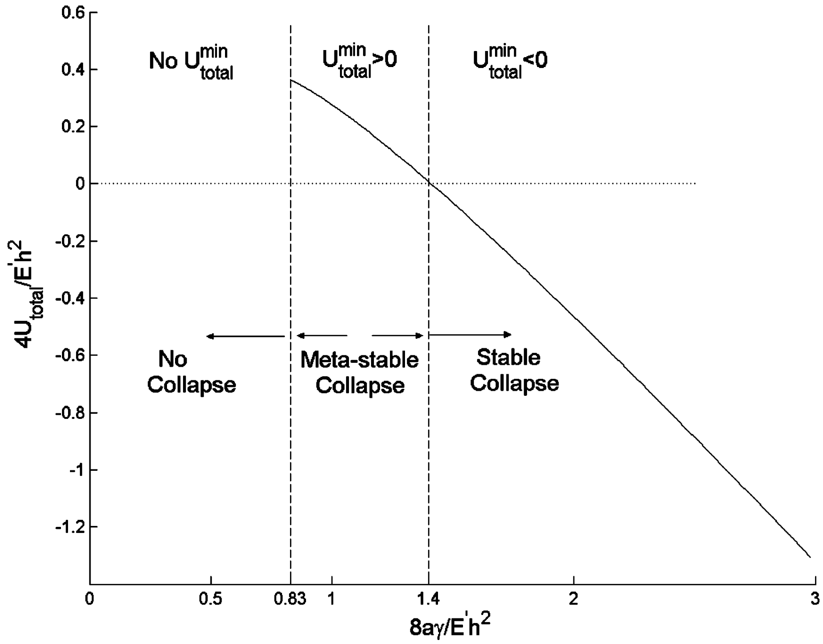

Figure 6. Minimal total potential energy, $U_{\text{total}}^{\min}$, normalized by $^1/_4E'h^2$, vs the normalized work of adhesion $8a\gamma/E'h^2$ for the limit of small punch spacing. Here $E' = {}^4/_3E$ is the plane-strain modulus of the PDMS stamp (E is Young's modulus), h and $2a$ are the punch height and spacing, respectively, and γ is the work of adhesion between the PDMS stamp and substrate. The horizontal dashed line represents the uncollapsed state ($U_{\text{total}} = 0$). The states of no collapse, metastable collapse, and stable collapse are governed by the normalized work of adhesion $8a\gamma/E'h^2$, which suggests a scaling law among the work of adhesion γ, stamp modulus E', and punch height h and spacing $2a$.

$2b$. The opening displacement can be obtained from Tada et al.[10] as

$$\Delta u_y = \begin{cases} 0, & |x| < b \\ h\left[1 - \dfrac{F\left(\sin^{-1}\sqrt{\dfrac{a^2-x^2}{a^2-b^2}}, \sqrt{1-\dfrac{b^2}{a^2}}\right)}{K\left(\sqrt{1-\dfrac{b^2}{a^2}}\right)}\right], & b < |x| < a \end{cases} \tag{10}$$

which rigorously satisfies $\Delta u_y|_{x=\pm b} = 0$ and $\Delta u_y|_{x=\pm a} = h$, where $F(\phi, k) = \int_0^\phi d\psi/\sqrt{1-k^2\sin^2\psi}$ is the incomplete elliptic integral of the first kind and $F(\pi/2, k) = K(k)$. Equation 10 can be used to compare with the experimentally measured opening displacement in the unsagged portion in order to validate the present model. The analysis of the shape of the collapsing roof will also give interesting insights into the adhesion forces.

The unsagged length in roof collapse (i.e., the length of the uncollapsed portion) is $L = a - b_{\text{critical}}$. The unsagged length can be measured from experiments, which provide a means to determine the work of adhesion between the stamp and substrate as to be shown in section 6. Figure 8 shows the unsagged length L, normalized by a, versus $1/(8a\gamma/E'h^2)$. The solid curve is obtained from Figure 7 by $L/a = 1 - b_{\text{critical}}/a$, and it holds for arbitrary $8a\gamma/E'h^2$. For $8a\gamma/E'h^2 \gg 1$, as shown in Appendix A, the unsagged length L has the asymptotic solution

$$L = \frac{1}{\pi}\frac{E'h^2}{8\gamma} \quad \text{if} \quad \frac{8a\gamma}{E'h^2} \gg 1 \tag{11}$$

This asymptotic solution corresponds to the straight dashed line in Figure 8, which merges to the solid curve for $8a\gamma/E'h^2 \gg 1$. For $8a\gamma/E'h^2$ on the order of 1, the asymptotic solution underestimates unsagged length L.

4. Periodic Punches: $2a \sim 2w$

An approximate solution for punch width $2w$ comparable to punch spacing (i.e., $2a \sim 2w$) is established in this section. It degenerates to the solution in section 3 in the limit $2a \ll 2w$. Each punch spacing is still modeled by a crack of length $2a$ with the center portion $2b$ collapsed, as shown in Figure 3. Similar to section 3, we do not account for the effect of elastic mismatch. Such an effect will be considered in section 5. Consequently, the results in section 5 can be compared with the experiments because PDMS and the substrate have a large elastic mismatch.

It is shown in Appendix B that the ratio of the deformation energy $U_{\text{deformation}}^{\text{periodic cracks}}$ for periodic cracks to the deformation energy $U_{\text{deformation}}^{\text{single cracks}}$ for a single crack is approximately given by

$$\frac{U_{\text{deformation}}^{\text{periodic cracks}}}{U_{\text{deformation}}^{\text{single cracks}}} \approx \frac{\pi^2}{8\left(1+\dfrac{w}{a}\right)^2 \ln\left[\sec\left(\dfrac{\pi}{2}\dfrac{1}{1+\dfrac{w}{a}}\right)\right]} \tag{12}$$

where sec = 1/cos. The above ratio approaches 1 at the limit of small punch spacing $w/a \to \infty$. It vanishes at the limit of small punch width $w/a \to 0$. The deformation energy for periodic cracks is obtained from eqs 12 and 7 as

$$U_{\text{deformation}}^{\text{periodic cracks}} \approx \frac{E'h^2}{4}\frac{K\left(\dfrac{b}{a}\right)}{K\left(\sqrt{1-\dfrac{b^2}{a^2}}\right)}\frac{\pi^2}{8\left(1+\dfrac{w}{a}\right)^2 \ln\left[\sec\left(\dfrac{\pi}{2}\dfrac{1}{1+\dfrac{w}{a}}\right)\right]} \tag{13}$$

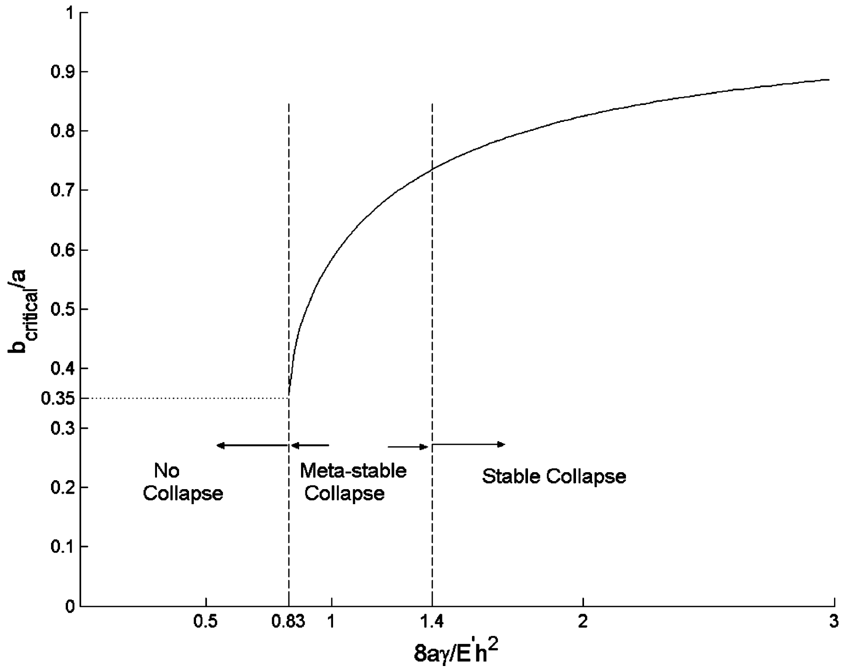

Figure 7. Normalized collapse length b_{critical}/a vs the normalized work of adhesion $8a\gamma/E'h^2$ for the limit of small punch spacing. Here $2b_{\mathrm{critical}}$ is the collapse length, $E' = {}^4/_3E$ is the plane-strain modulus of the PDMS stamp (E is Young's modulus), $2a$ and h are the punch spacing and height, respectively, and γ is the work of adhesion between the PDMS stamp and substrate. The states of no collapse, metastable collapse, and stable collapse are governed by the normalized work of adhesion $8a\gamma/E'h^2$, which suggests a scaling law among the work of adhesion γ, stamp modulus E', and punch height h and spacing $2a$.

The total potential energy in eq 8 then becomes

$$U_{\mathrm{total}} = \frac{E'_{\mathrm{eff}}h^2}{4}\left[\frac{K\left(\frac{b}{a}\right)}{K\left(\sqrt{1-\frac{b^2}{a^2}}\right)} - \frac{8a\gamma}{E'_{\mathrm{eff}}h^2}\frac{b}{a}\right] \tag{14}$$

where E'_{eff} is given in terms of plane-strain modulus E' of the stamp and punch width/spacing ratio w/a by

$$E'_{\mathrm{eff}} = E'\frac{\pi^2}{8\left(1+\frac{w}{a}\right)^2 \ln\left[\sec\left(\frac{\pi}{2}\frac{1}{1+\frac{w}{a}}\right)\right]} \tag{15}$$

Equation 14 is identical to eq 8 except that (plane-strain) stamp modulus E' is replaced by E'_{eff} in eq 15, which depends on w/a. The normalized work of adhesion $8a\gamma/E'h^2$ for a single crack now becomes

$$\frac{8a\gamma}{E'_{\mathrm{eff}}h^2} = \frac{8a\gamma}{E'h^2}\frac{8}{\pi^2}\left(1+\frac{w}{a}\right)^2 \ln\left[\sec\left(\frac{\pi}{2}\frac{1}{1+\frac{w}{a}}\right)\right] \tag{16}$$

for periodic cracks. The relation between total potential energy U_{total} and collapse length b shown in Figure 5 still holds if $8a\gamma/E'h^2$ is replaced by $8a\gamma/E'_{eff}h^2$.

Collapse length $2b_{\mathrm{critical}}$, determined by minimizing U_{total} in eq 14, and the corresponding minimal total potential energy $U_{\mathrm{total}}^{\mathrm{min}}$ are the same as those in Figures 7 and 6, respectively, if $8a\gamma/E'h^2$ is replaced by $8a\gamma/E'_{\mathrm{eff}}h^2$. To illustrate the effect of punch width/spacing ratio w/a, we show that the normalized minimal total potential energy $4U_{\mathrm{total}}^{\mathrm{min}}/E'h^2$ versus the normalized work of adhesion $8a\gamma/E'h^2$ (not $8a\gamma/E'_{\mathrm{eff}}h^2$!) for $w/a = 0.1$, 0.5, 1, 5, and ∞ in Figure 9, where $w/a = \infty$ corresponds to the limit of small punch spacing in section 3. It is observed that as punch width/spacing ratio w/a decreases the curve separating collapse/no collapse shifts to the left (i.e., roof collapse becomes easier because of the interaction among punches). Furthermore, the curve for $w/a = 5$ is essentially the same as that for $w/a = \infty$, which means that the interaction effect among punches disappears once the punch width is about 5 times the punch spacing. The horizontal line in Figure 9 still separates the stable and metastable collapse.

Figure 10 shows the normalized collapse length b_{critical}/a versus the normalized work of adhesion $8a\gamma/E'h^2$ (not $8a\gamma/E'_{\mathrm{eff}}h^2$!) for punch width/spacing ratio $w/a = 0.1$, 0.5, 1, 5, and ∞. Once again, the curves for $w/a = 5$ and ∞ are essentially the same. As w/a decreases, the normalized collapse length b_{critical}/a increases (i.e., larger collapse length due to the interaction among punches). The two horizontal dashed lines in Figure 10, which correspond to $b_{\mathrm{critical}}/a = 0.35$ and 0.74, still separate the collapse/no collapse and stable collapse/metastable collapse, respectively.

5. Effect of Elastic Mismatch between the Stamp and Substrate

It is important to note that the analyses in sections 3 and 4 have not accounted for the mismatch in the elastic moduli between the stamp and substrate. Such an effect is considered in this section, and the results can then be compared with the experiments.

For a crack in an elastic homogeneous material of PDMS, crack tip energy release rate G is related to mode-I stress intensity factor K_{I} by

$$G = \frac{K_{\mathrm{I}}^2}{E'} \tag{17}$$

where E' is the plane-strain modulus of PDMS. For a crack

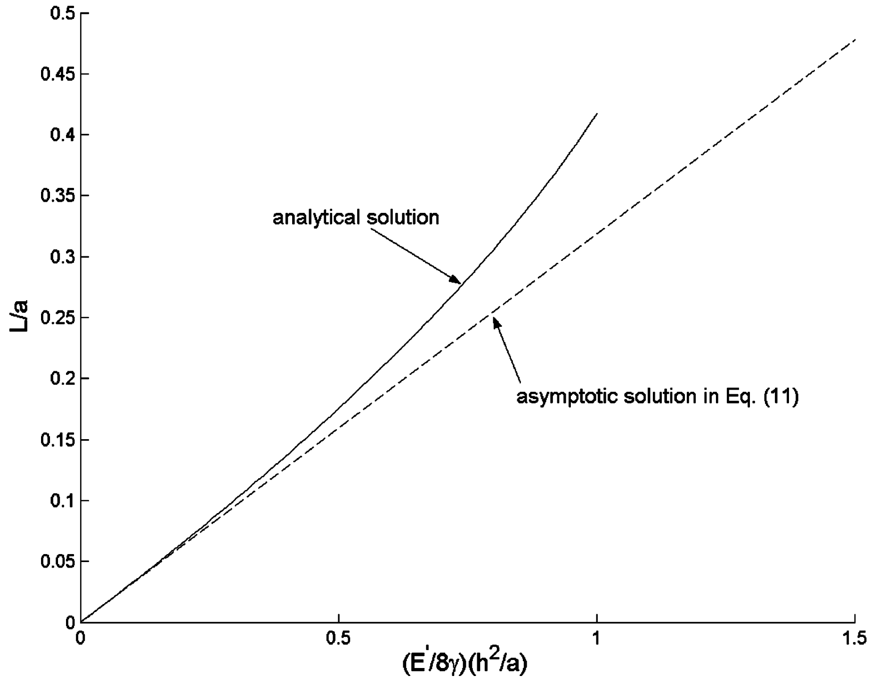

Figure 8. Unsagged length L, normalized by half of the punch spacing a, vs $E'h^2/8a\gamma$ for the limit of small punch spacing. Here $E' = {}^4\!/_3E$ is the plane-strain modulus of the PDMS stamp (E is Young's modulus), h is the punch height, and γ is the work of adhesion between the PDMS stamp and substrate. The straight dashed line represents the asymptotic solution in eq 11, and the solid curve corresponds to the analytical solution.

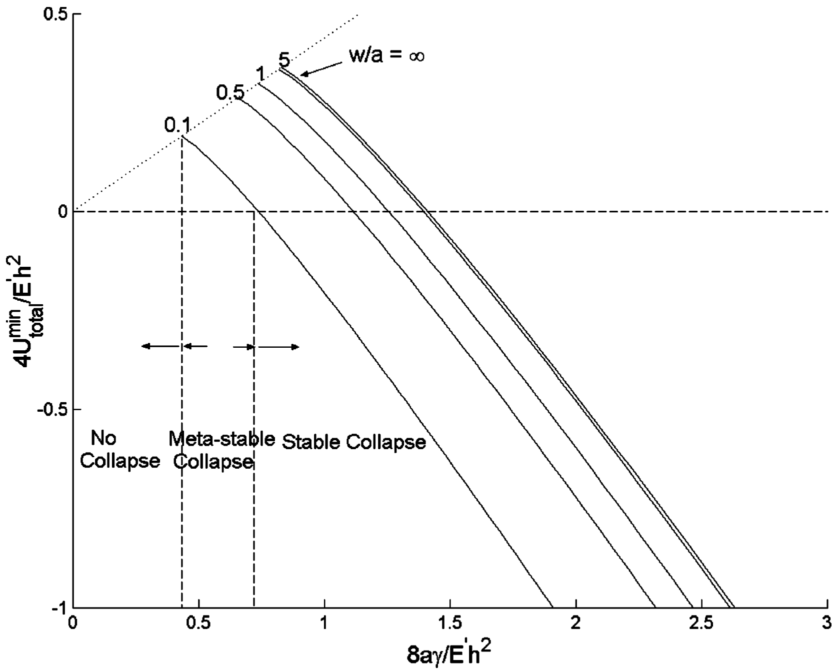

Figure 9. Minimal total potential energy, $U_{\text{total}}^{\min}$, normalized by ${}^1\!/_4E'h^2$, vs the normalized work of adhesion $8a\gamma/E'h^2$ for the punch width/spacing ratio $w/a = \infty$, 5, 1, 0.5, and 0.1, where $w/a = \infty$ corresponds to the limit of small punch spacing shown in Figure 6, $E' = {}^4\!/_3E$ is the plane-strain modulus of the PDMS stamp (E is Young's modulus), h, $2a$, and $2w$ are the punch height, spacing, and width, respectively, and γ is the work of adhesion between the PDMS stamp and substrate. The horizontal dashed line represents the uncollapsed state ($U_{\text{total}} = 0$). The states of no collapse, metastable collapse, and stable collapse governed by the normalized work of adhesion $8a\gamma/E'h^2$ and the punch width/spacing ratio w/a are shown only for $w/a = 0.1$ by the vertical dashed lines.

on the interface between PDMS and the substrate, the crack tip energy release rate becomes[11]

$$G = \frac{1}{2\cosh^2(\pi\epsilon)}\left(\frac{1}{E'} + \frac{1}{E'_{\text{substrate}}}\right)|K|^2 \qquad (18)$$

where $|K|$ is the amplitude of complex stress intensity factor K for the bimaterial interface crack tip, E' and $E'_{\text{substrate}}$ are the (plane-strain) moduli of PDMS and the substrate, respectively, and bimaterial parameter ϵ is related to shear modulus μ and Poisson's ratio ν of PDMS and their counterparts $\mu_{\text{substrate}}$ and $\nu_{\text{substrate}}$ for

(11) Rice, J. R. *J. Appl. Mech.* **1988**, *55*, 98−103.

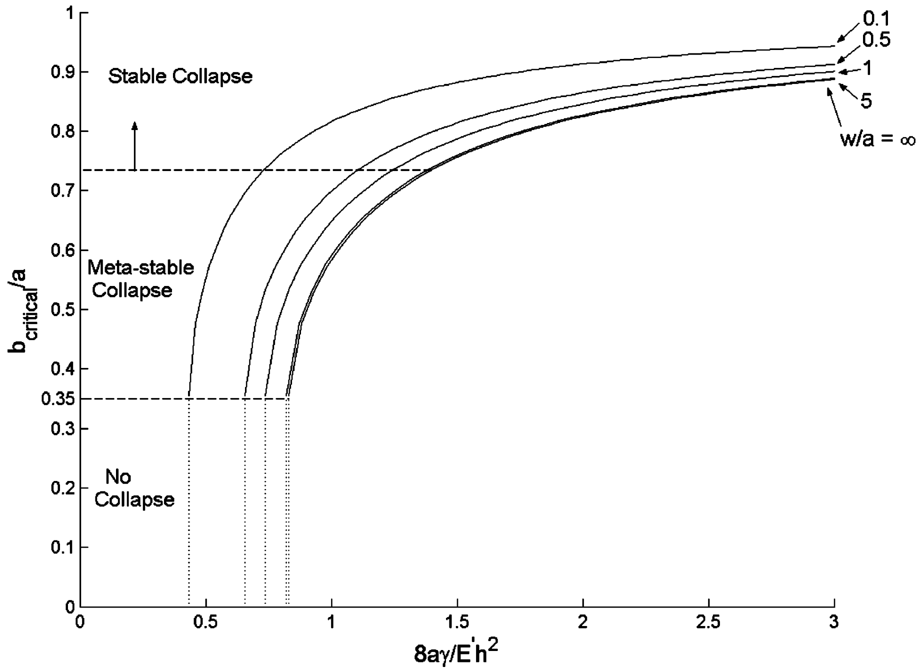

Figure 10. Normalized collapse length b_{critical}/a versus normalized work of adhesion $8a\gamma/E'h^2$ for the punch width/spacing ratio $w/a = \infty$, 5, 1, 0.5, and 0.1, where $w/a = \infty$ corresponds to the limit of small punch spacing shown in Figure 7, $E' = {}^4/_3E$ is the plane-strain modulus of the PDMS stamp (E is Young's modulus), $2b_{\text{critical}}$ is the collapse length, h, $2a$, and $2w$ are the punch height, spacing, and width, respectively, and γ is the work of adhesion between the PDMS stamp and substrate. The states of no collapse, metastable collapse, and stable collapse are governed by the normalized work of adhesion $8a\gamma/E'h^2$ and punch width/spacing ratio w/a.

the substrate by

$$\epsilon = \frac{1}{2\pi}\ln\left[\frac{\dfrac{3-4\nu}{\mu} + \dfrac{1}{\mu_{\text{substrate}}}}{\dfrac{3-4\nu_{\text{substrate}}}{\mu_{\text{substrate}}} + \dfrac{1}{\mu}}\right] \tag{19}$$

The PDMS is incompressible ($\nu = 0.5$), and its elastic moduli $E'$and μ ($\sim$1 MPa) are orders of magnitude smaller than the elastic moduli of the substrate (e.g., silicon or silica with moduli on the order of 100 GPa). These give a vanishing bimaterial parameter ϵ in eq 19 (i.e., $\epsilon = 0$). The energy release rate in eq 18 now becomes

$$G = \frac{1}{2E'}|K|^2 \tag{20}$$

There exist several analytical solutions for bimaterial interface cracks.[11−13] All of these analytical solutions show that for the vanishing bimaterial parameter, $\epsilon = 0$, stress intensity factor $|K|$ is the same as its counterpart K_I in homogeneous materials, $|K| = K_I$. The energy release rate in eq 20 for an interface crack tip between PDMS and the substrate is then related to that in eq 17 for a crack tip in the homogeneous PDMS by replacing PDMS modulus E' with $2E'$. In other words, the effect of elastic mismatch between PDMS and the substrate on the crack tip energy release rate can be accounted for if the solution for homogeneous material in sections 3 and 4 is modified by replacing E' with $2E'$. For example, deformation energy $U_{\text{deformation}}$ in eq 7 for the limit of small punch spacing $2a \ll 2w$ in section 3 now becomes

$$U_{\text{deformation}} = \frac{(2E')h^2}{4}\frac{K\left(\dfrac{b}{a}\right)}{K\left(\sqrt{1-\dfrac{b^2}{a^2}}\right)} \tag{21}$$

The above expression can also be obtained from a simple mechanics argument. Because the substrate is several orders of magnitude stiffer than PDMS, it hardly deforms such that the opening displacement h is completely imposed on the PDMS. This is in contrast to the analyses in sections 3 and 4 for the homogeneous material where the material on each side of the crack undergoes one-half of the opening displacement, $h/2$. In other words, opening displacement h in sections 3 and 4 needs to be replaced by $2h$, which gives the deformation energy as

$$U_{\text{deformation}} = \frac{1}{2}\frac{E'(2h)^2}{4}\frac{K\left(\dfrac{b}{a}\right)}{K\left(\sqrt{1-\dfrac{b^2}{a^2}}\right)}$$

where the factor of 1/2 comes from half of the material (PDMS). This expression is identical to that in eq 21.

The adhesion energy $2b\gamma$ remains the same. Therefore, the normalized work of adhesion $8a\gamma/E'h^2$ is replaced by $8a\gamma/(2E')h^2 = 4a\gamma/E'h^2$ after the effect of elastic mismatch is accounted for

$$\frac{8a\gamma}{E'h^2} \Rightarrow \frac{4a\gamma}{E'h^2} \tag{22}$$

For the limit of small punch spacing $2a \ll 2w$ in section 3, the criterion governing stamp collapse onto

(12) Rice, J. R.; Sih, G. C. *J. Appl. Mech.* **1965**, *32*, 418−423.
(13) Hutchinson J. W.; Suo, Z. *Adv. Appl. Mech.* **1992**, *29*, 63−191.

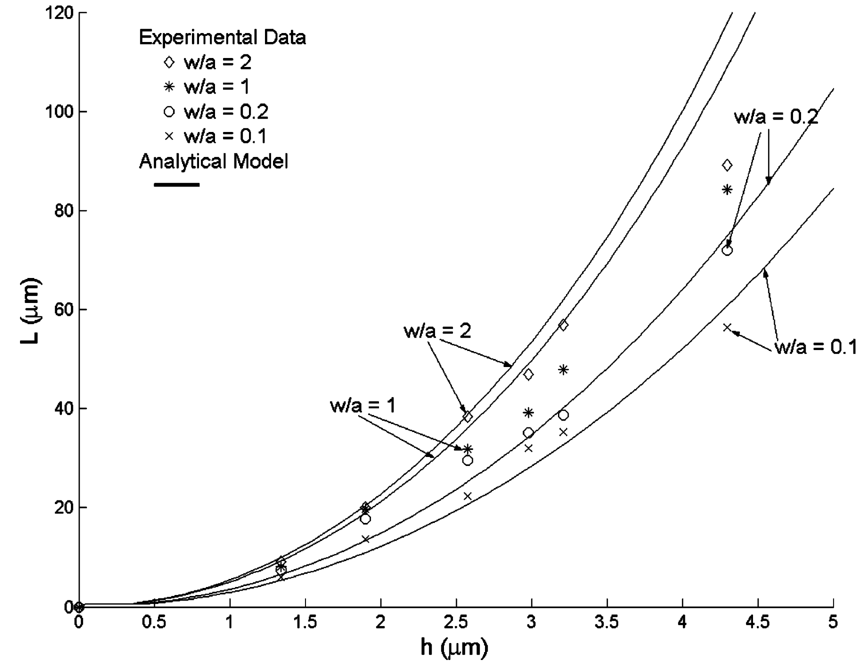

Figure 11. Unsagged length L versus punch height h for the PDMS stamp on the substrate. The present analytical model is compared with the experimental data for punch width/spacing ratio $w/a = 2$, 1, 0.2, and 0.1. The plane-strain elastic modulus of PDMS is $E' = 3.73$ MPa. The punch spacing is $2a = 1$ mm. The work of adhesion is $\gamma = 50.6$ mJ/m^2.

the substrate becomes

$$
\begin{aligned}
&\text{no collapse} && \text{if } \frac{4a\gamma}{E'h^2} < 0.83\\
&\text{metastable collapse} && \text{if } 0.83 < \frac{4a\gamma}{E'h^2} < 1.40\\
&\text{stable collapse} && \text{if } 1.40 < \frac{4a\gamma}{E'h^2}
\end{aligned} \tag{23}
$$

For periodic punches in section 4 (i.e., $a \sim w$), the criterion governing stamp collapse onto the substrate becomes

$$
\begin{aligned}
&\text{no collapse}\\
&\quad \text{if } \frac{4a\gamma}{E'h^2}\frac{8}{\pi^2}\left(1+\frac{w}{a}\right)^2 \ln\left[\sec\left(\frac{\pi}{2}\frac{1}{1+\frac{w}{a}}\right)\right] < 0.83\\
&\text{metastable collapse}\\
&\quad \text{if } 0.83 < \frac{4a\gamma}{E'h^2}\frac{8}{\pi^2}\left(1+\frac{w}{a}\right)^2 \ln\left[\sec\left(\frac{\pi}{2}\frac{1}{1+\frac{w}{a}}\right)\right] < 1.40\\
&\text{stable collapse}\\
&\quad \text{if } 1.40 < \frac{4a\gamma}{E'h^2}\frac{8}{\pi^2}\left(1+\frac{w}{a}\right)^2 \ln\left[\sec\left(\frac{\pi}{2}\frac{1}{1+\frac{w}{a}}\right)\right]
\end{aligned} \tag{24}
$$

The above equation, accounting for the effects of both elastic mismatch and multiple punches, separates these three states. In particular, the criterion for no collapse can be rewritten as

$$\frac{a\gamma}{Eh^2}\left(1+\frac{w}{a}\right)^2 \ln\left[\sec\left(\frac{\pi}{2}\frac{1}{1+\frac{w}{a}}\right)\right] < 0.35 \tag{24a}$$

where h, $2a$, and $2w$ are the punch height, spacing, and width, respectively, E is the Young's modulus (not plane-strain modulus E') of the PDMS stamp, and γ is the work of adhesion between the PDMS stamp and substrate.

The unsagged length for the limit of $4a\gamma/E'h^2 \gg 1$, accounting for the interactions among multiple punches and the elastic mismatch between the PDMS stamp and substrate, is given in Appendix A.

6. Comparison with Experiments

In this section, we compare the analytical results in section 5 with the experimental data in order to determine the work of adhesion γ between the stamp and substrate and to validate the present analytical models. In the following, we provide some details on processing specimen and experimental observations.

The masters used to fabricate the PDMS stamps were prepared using test-grade silicon wafers (Montco Silicon Technologies, www.silicon-wafers.com) and positive photoresist (Shipley, www.shipley.com) using conventional contact mode photolithography process. They were then coated with a nonstick fluorosilane ((tridecafluoro-1,1,2,2-tetrahydrooctyl)-1-trichlorosilane) self-assembled monolayer to facilitate the release of the PDMS stamps. PDMS (Sylgard 184 from Dow Corning, www.dowcorning.com) was mixed (10:1 ratio) and degassed, poured over the masters, and cured in an oven at 80 °C. For the sagging experiments, test-grade silicon wafers were cleaned with acetone, 2-propanol, and deionized water and then dried on a hot plate at 150 °C for 10 min.

The experiments[9] were conducted by placing the patterned stamps on a substrate of silicon wafer with a native silica glass layer. The PDMS stamps have periodic, rectangular grooves and flat punches. The length of the grooves in the out-of-plane direction is a few centimeters. The grooves were observed to collapse onto the substrate. The contact part of the collapsed region always took a significant portion of the groove and did not change even if we turned the experimental setup upside down. Unsagged length L was measured in the experiments.

Figure 11 shows unsagged length L versus punch height h for several punch width/spacing ratios w/a obtained from the experiments of the PDMS stamp on a silicon wafer with a thin silica coating. The elastic modulus of PDMS is $E = 2.8$ MPa,[9] which gives plane-strain modulus $E' = 3.73$ MPa because PDMS is incompressible ($\nu = 0.5$). This plane-strain modulus falls into the range (3.5−4.5 MPa) reported by Sharp et al.[8] The punch spacing is fixed at $2a = 1$ mm ($= 1000$ μm). Punch width $2w$ ranges from 100 μm to 2 mm($= 2000$ μm). The work of adhesion γ is determined from the experimental data for $w/a = 0.1$, which gives

$$\frac{\gamma}{E'} = 0.0136\ \mu\text{m} \tag{25}$$

Here, unsagged length L is calculated from b_{critical}/a in Figure 10 accounting for the effect of elastic mismatch. For $E' = 3.73$ MPa of PDMS, the work of adhesion is

$$\gamma = 50.6\ \text{mJ/m}^2 \tag{26}$$

This value is on the same order of magnitude with that reported by Chaudhury and Whitesides.[14]

On the basis of the work of adhesion given above, we have calculated unsagged length L versus punch height h for $w/a = 0.2$, 1, and 2. The results are shown in Figure 11 together with the experimental data. The analytical model agrees reasonably well with the experimental data for a wide range of w/a.

In the following, we discuss the effect of gravity, which has been neglected in prior sections. Hui et al.[7] provided an estimate for the maximum deflection of the punch due to uniform remote compression σ_0. The effect of gravity can be estimated by taking $\sigma_0 = \rho g H$, where ρ is the mass density of PDMS ($= 950$ kg/m^3), $g = 9.8$ m/s^2 is the gravity acceleration, and H is the height of the PDMS layer (not the punch). For the above representative value of punch spacing $2a = 1$ mm, punch width $2w = 100$ μm, plane-strain modulus $E' = 3.73$ MPa, and a large height $H = 10$ mm of the PDMS layer, the maximum displacement due to gravity is several tens of nanometer. This value is much smaller than the minimal punch height ($h = 1.34$ μm) such that the effect of gravity is insignificant in the present study of soft lithography.

7. Concluding Remarks and Discussion

We have studied the so-called roof collapse in soft lithography due to the adhesion between the PDMS stamp and substrate. The effects of multiple punches on the stamp, as well as the elastic mismatch between the PDMS stamp and substrate, are accounted for. It is shown that roof collapse is governed by two nondimensional parameters, $8a\gamma/E'h^2$ and w/a, where $E' = 4/3\ E$ is the plane-strain modulus of the PDMS stamp (E is the Young's modulus), γ is the work of adhesion between the stamp and substrate, $2a$ is the punch spacing, h is the punch height, and $2w$ is the punch width. The normalized work of adhesion $8a\gamma/E'h^2$ suggests an important scaling law among the stamp modulus, punch height and spacing, and work of adhesion between the PDMS stamp and substrate. Three regimes of roof collapse are identified, namely, no collapse for weak adhesion, metastable collapse for intermediate adhesion, and stable collapse for strong adhesion. A simple criterion separating these three regimes is established. The present model also predicts the unsagged length in roof collapse, which agrees well with the experimental data.

It is discussed in section 2 that the work of adhesion γ is given by

$$\gamma = \gamma_{\text{PDMS/air}} + \gamma_{\text{substrate/air}} - \gamma_{\text{PDMS/substrate}} \tag{27}$$

where $\gamma_{\text{PDMS/air}}$ and $\gamma_{\text{substrate/air}}$ are the surface energy of PDMS and the substrate, respectively, and $\gamma_{\text{PDMS/substrate}}$ is the interfacial energy. Once there is liquid between PDMS and the substrate, the above expression becomes $\gamma = \gamma_{\text{PDMS/liquid}} + \gamma_{\text{substrate/liquid}} - \gamma_{\text{PDMS/substrate}}$. For rubber in air and in water, Johnson et al.'s[15] experiments showed that $\gamma_{\text{rubber/liquid}}$ is an order of magnitude smaller than $\gamma_{\text{rubber/air}}$. If such properties also hold for PDMS (i.e., $\gamma_{\text{PDMS/air}} \gg \gamma_{\text{PDMS/liquid}}$), then the work of adhesion γ becomes smaller once there is liquid between PDMS and the substrate, which makes it more difficult for roof collapse in soft lithography.

Acknowledgment. We acknowledge financial support from the NSF through Nano-CEMMS (grant no. DMI 03-28162) at the University of Illinois. Y.Y.H. also acknowledges support from the NSFC.

Appendix A

We consider the limit $8a\gamma/E'h^2 \gg 1$, which corresponds to a large punch spacing (or equivalently a compliant stamp and a short punch or strong stamp/substrate adhesion). Under such a limit, collapse length $2b_{\text{critical}}$ approaches punch spacing $2a$ (Figure 7). The total potential energy in eq 8 then takes the asymptotic form

$$U_{\text{total}} = \frac{E'h^2}{4}\left[\frac{1}{\pi}\ln\frac{a}{L} - \frac{8a\gamma}{E'h^2}\left(1 - \frac{L}{a}\right) + O(1)\right] \tag{A1}$$

where we have used the limits $K(0) = \pi/2$ and $K(k \to 1) = -{}^1\!/_2 \ln(1-k) + O(1)$ and $O(1)$ represents the terms that remain bounded in the limit of $b_{\text{critical}}/a \to 1$ (or equivalently $L/a \to 0$).

Equation 4 can be equivalently written as $\partial U_{\text{total}}/\partial L = 0$. Its solution is obtained analytically for $8a\gamma/E'h^2 \gg 1$ and is given in eq 11.

For periodic punches with $4a\gamma/E'h^2 \gg 1$, the unsagged length in eq 11 becomes

$$L = \frac{1}{\pi}\frac{E'_{\text{eff}}h^2}{4\gamma} = \frac{1}{\pi}\frac{E'h^2}{4\gamma}\frac{\pi^2}{8\left(1+\dfrac{w}{a}\right)^2\ln\left[\sec\left(\dfrac{\pi}{2}\dfrac{1}{1+\dfrac{w}{a}}\right)\right]} \quad \text{if } \frac{4a\gamma}{E'h^2} \gg 1 \tag{A2}$$

Here we have accounted for the interactions among multiple punches and the elastic mismatch between the PDMS stamp and substrate.

Appendix B

There is no analytical solution for the coplanar, periodic cracks (of length $2a$) shown in Figure 3 that are subject to a constant crack-opening displacement h over a central portion (of length $2b$) on each crack. Let $U_{\text{deformation}}^{\text{periodic cracks}}$ denote the deformation energy for such a problem and $U_{\text{deformation}}^{\text{single cracks}}$ denote the deformation energy for a single crack subject to a constant crack-opening displacement over a central portion of the crack. We approximate their

(14) Chaudhury, M. K.; Whitesides, G. M. *Langmuir* **1991**, *7*, 1013−1025.

(15) Johnson, K. L.; Kendall, K.; Roberts, A. D. *Proc. R. Soc. London, Ser. A* **1971**, *324*, 301−313.

ratio by its counterpart for periodic cracks and a single crack subject to uniform normal traction on crack faces because analytical solutions exist for the latter.

For the single crack (crack length $2a$) subject to the uniform normal traction $\sigma^{\text{single crack}}$, the crack-opening displacement is given by[10]

$$\Delta u_y^{\text{single crack}} = \frac{4\sigma^{\text{single crack}}}{E'}\sqrt{a^2 - x^2} \qquad \text{(B1)}$$

The deformation energy is given by

$$\frac{1}{2}\int_{-a}^{a} \sigma^{\text{single crack}}\Delta u_y^{\text{single crack}}\, \mathrm{d}x = \frac{(\sigma^{\text{single crack}})^2 \pi a^2}{E'} \qquad \text{(B2)}$$

For periodic cracks (crack length $2a$, spacing $2w$) subject to uniform traction $\sigma^{\text{periodic cracks}}$, the opening displacement becomes[10]

$$\Delta u_y^{\text{periodic cracks}} = \frac{4\sigma^{\text{periodic cracks}}}{E'}\,\frac{2(a+w)}{\pi}\cosh^{-1}\left(\frac{\cos\dfrac{\pi x}{2(a+w)}}{\cos\dfrac{\pi a}{2(a+w)}}\right) \qquad \text{(B3)}$$

The corresponding deformation energy is given by

$$\frac{1}{2}\int_{-a}^{a} \sigma^{\text{periodic cracks}}\Delta u_y^{\text{periodic cracks}}\, \mathrm{d}x = \frac{(\sigma^{\text{periodic cracks}})^2 \pi a^2}{E'}\,\frac{8}{\pi^2}\left(1+\frac{w}{a}\right)^2 \ln\left[\sec\left(\frac{\pi}{2}\,\frac{1}{1+\frac{w}{a}}\right)\right] \qquad \text{(B4)}$$

Normal tractions $\sigma^{\text{single crack}}$ and $\sigma^{\text{periodic cracks}}$ are related by requiring that the periodic cracks and single crack have the same displacement in order to represent punch height h. This is enforced in an average sense

$$\frac{1}{2a}\int_{-a}^{a} \Delta u_y^{\text{single crack}}\, \mathrm{d}x = \frac{1}{2a}\int_{-a}^{a} \Delta u_y^{\text{periodic cracks}}\, \mathrm{d}x \qquad \text{(B5)}$$

The substitution of eqs B1 and B3 into B5 yields

$$\frac{\sigma^{\text{periodic cracks}}}{\sigma^{\text{single crack}}} = \frac{\pi^2}{8\left(1+\frac{w}{a}\right)^2 \ln\left[\sec\left(\frac{\pi}{2}\,\frac{1}{1+\frac{w}{a}}\right)\right]} \qquad \text{(B6)}$$

The ratio of deformation energy in eq B4 for periodic cracks to that in eq B2 for a single crack then leads to eq 12.

LA0502185